European Journal of Pharmaceutical Sciences 187 (2023) 106484

Contents lists available at ScienceDirect

European Journal of Pharmaceutical Sciences

journal homepage: www.elsevier.com/locate/ejps

Design and in vitro assessment of chitosan nanocapsules for the pulmonary delivery of rifabutin*

Lorena Valverde-Fraga [a,b], Razan Haddad [b,c], Nasr Alrabadi [c], Sandra Sánchez [d], Carmen Remuñán-López [a,e], Noemi Csaba [a,b,*]

[a] Nanobiofar Group, Department of Pharmacology, Pharmacy & Pharmaceutical Technology, Faculty of Pharmacy, University of Santiago de Compostela Campus Vida, 15782 Santiago de Compostela, Spain
[b] Center for Research in Molecular Medicine and Chronic Diseases (CiMUS), University of Santiago de Compostela Campus Vida, 15782 Santiago de Compostela, Spain
[c] Department of Pharmaceutical Technology and Pharmaceutical Sciences, Faculty of Pharmacy, Department of Pharmacology, Faculty of Medicine, Jordan University of Science and Technology, Irbid 22110, Jordan
[d] Department of Microbiology and Parasitology, Faculty of Pharmacy, University of Santiago de Compostela Campus Vida, 15782 Santiago de Compostela, Spain
[e] Institute of Materials (iMATUS), University of Santiago de Compostela, 15782 Santiago de Compostela, Spain

ARTICLE INFO

Keywords:
Chitosan nanocapsules
Rifabutin
PEG-stearate
Lecithin
Antituberculosis treatment

ABSTRACT

Tuberculosis (TB) is a life-threatening disease and a main cause of death worldwide. It mainly affects the lungs, and it is attributed to the infection with *Mycobacterium tuberculosis* (MTB). Current treatments consist of the oral administration of combinations of antibiotics including rifabutin, in high doses and for long periods of time. These therapeutic regimens are associated with many side effects and high rates of drug resistance. To overcome these problems, this study aims at developing a nanosystem for the improved delivery of antibiotics, with potential application in pulmonary delivery.

Chitosan-based nanomaterials are widely used in biomedical applications, due to their biodegradability and biocompatibility, as well as their potential antimicrobial effects and lack of toxicity. In addition, this polymer is particularly attractive for mucosal delivery due to its bioadhesive properties. Therefore, the structure of the proposed nanocarrier consists of a chitosan shell and a lipid core with a combination of different oils and surfactants to allow optimal association of the hydrophobic drug rifabutin. These nanocapsules were characterized in terms of size, polydispersity index, surface charge, morphology, encapsulation efficiency and biological stability. The release kinetics of the drug-loaded nanostructures was evaluated in simulated lung media. Moreover, in vitro studies in different cell models (A549 and Raw 264.7 cells) demonstrated the safety of the nanocapsules as well as their efficient internalization. An antimicrobial susceptibility test was performed to evaluate the efficacy of the rifabutin-loaded nanocapsules against *Mycobacterium phlei*. This study indicated complete inhibition for antibiotic concentrations within the expected susceptibility range of *Mycobacterium* ($\leq$ 0.25–16 mg/L).

1. Introduction

Tuberculosis (TB) is a life-threatening disease that is classified by the WHO as one of the top 10 worldwide causes of death from a single infectious agent. It affects mainly the lungs, and it is attributed to the infection by *Mycobacterium tuberculosis* (MTB) (Andersen et al., 2007; World Health Organization, 2022). The continued spreading and survival of MTB depends on the airborne transmission among humans. The disease has broadened its burden by developing several strains with different types of resistances, such as Multi-drug resistance (MDR), Single-drug resistance (SDR), and Extensive drug resistance (XDR) strains (Kaur et al., 2016). Generally, TB is classified as being either latent or active. Latent TB refers to the situation where the bacteria are immobile but present in the body, the disease is not active, and the patient has no signs or symptoms. In the status of active TB, the bacteria become virulent, the patients show signs or symptoms of sickness, and the disease is sanitarily communicable (Kaur et al., 2016).

Rifabutin is one of the agents used in the treatment of TB (Rifabutin Uses, 2022). It works through the inhibition of DNA-dependent RNA synthesis in prokaryotes. Owing to its high volume of distribution,

* "Created with BioRender.com"

* Corresponding author.
E-mail address: noemi.csaba@usc.es (N. Csaba).

https://doi.org/10.1016/j.ejps.2023.106484
Received 17 February 2023; Received in revised form 9 May 2023; Accepted 30 May 2023
Available online 31 May 2023

rifabutin concentrates properly in the lung and penetrates highly intracellularly (Sousa et al., 2008). Moreover, it has an active metabolite, 25-O-desacetyl rifabutin (des-rifabutin), which doesn't stimulate CYP3A and glucuronosyltransferases as other antimycobacterial drugs such as rifampicin do and, thus have less drug-drug interactions (Burman and Gallicano, 2001; Brainard et al., 2011). Consequently, in 2009, the WHO involved rifabutin in the List of Essential Medicines for the treatment of some TB patients (Rockwood et al., 2019). In these cases, rifabutin is daily administered orally in combination with other antibiotics in high doses and for prolonged time periods, causing several side effects, such as discoloration of the skin, tears, sweat, saliva, urine, or stools. It can also cause gas, burping, upset stomach, rash, and muscle pain (Rifabutin Uses, 2022).

Although the oral route of anti-TB drugs is still commonly effective and recommended for the treatment of TB, the associated side effects sometimes become severe and hence, affect the patients' compliance. Besides, there are also high ratings of drug resistance, which further restricts the efficacy of the treatment. Consequently, it is urgent to develop new therapeutic agents as well as new administration procedures and delivery strategies for the existing therapeutic drugs, to overcome these circumstances.

In this regard, there are obvious benefits of administering the drugs directly to the lung; using adequate inhalation delivery systems and to target the drug to the alveolar macrophages holding the MTB and hence decreasing the risk of systemic toxicities and enhancing the patient's compliance (Pandey and Khuller, 2005). Additionally, as drug resistance correlates with the exposure of a bacteria to subtherapeutic levels of antibiotics, the use of a suitable drug carrier system that provides superior concentrations of antibiotics at the site of bacterial multiplication and growth, would enhance the bactericidal effect and reduce the development of resistant strains. As MTB multiplies and grows within-host mononuclear phagocytes, the encapsulation of antitubercular agents inside particulate carriers could provide a potent tool for specific targeting and accumulation within the infected cells. Furthermore, these carriers can enhance the penetration of hydrophobic antitubercular/antimycobacterial drugs and protect them from degradation or elimination before reaching the infected tissues (Pandey and Ahmad, 2011; Clemens et al., 2012).

Various inhaled delivery systems for the treatment of TB have been proposed to overcome the obstacles related to the oral route and improve the amounts of antitubercular agents directly reaching the infection sites, such as microparticles, liposomes and nanoparticles (Pai et al., 2016; Gaspar et al., 2016, 2017; Pinheiro et al., 2011). Chitosan is a cationic polysaccharide derived from the deacetylation of chitin and is a widely distributed polymer that can be obtained from various resources such as crustacean shells like crabs and shrimps (Rinaudo, 2006). Due to its abundant availability, mucoadhesiveness, biodegradability, biocompatibility, low immunogenicity, and inherent pharmacological properties, chitosan has multiple and favorable applications in pharmaceutical and biomedical fields (Rinaudo, 2006; Kean and Thanou, 2010). Moreover, the absence of chitosan toxicity in lung epithelial cell lines and *in vivo* has been recognized previously (Huang et al., 2007; Grenha et al., 2007; Aranaz et al., 2012). As well, chitosan has achieved great attention in the development of nanostructured drug delivery systems involving colon-targeting, cancer therapy, mucosal, vaccine, gene, nasal, and pulmonary delivery (Illum, 1998; Dodane and Vilivalam, 1998).

Chitosan is widely recognized for its potential antimicrobial activity, while exhibiting low toxicity to mammalian cells. Recently it has been proposed as a new generation antimicrobial agent with the capacity to control a wide variety of microorganisms, including antibiotic resistant pathogens (Costa et al., 2014; Jeon et al., 2014; Khan et al., 2020). Although the antimicrobial mechanism of action of chitosan is not completely understood, it is well established that the molecular structure of chitosan is a prerequisite for this specific effect. It has been suggested that a positive charge on the amine group of the glucosamine monomer at low pH allows interaction with negatively charged microbial cell membranes, leading to the leakage of intracellular constituents (Liu et al., 2004). In addition, chitosan nanocapsules are endowed with favorable characteristics such as large surface-to-volume ratio, great capacity for drug loading and possibility of functionalization. It is also expected that bacterial cells are more affected by polycationic chitosan nanostructures than pure chitosan alone (Rashki et al., 2021). Recently it has been reported that chitosan interferes with quorum sensing responses and biofilm formation in various Gram-positive and negative bacteria. In this sense, it is important to emphasize that chitosan nanostructures like nanoparticles and nanocapsules can satisfactorily maintain the quorum sensing activity of free chitosan (Qin et al., 2017; Vila-Sanjurjo et al., 2019). Considering this, rifabutin was formulated in a nanocarrier based on chitosan nanocapsules. More specifically, in this work, we have prepared different rifabutin-loaded chitosan- nanocapsules and characterized them in vitro and in cell culture to overcome the challenges associated with the oral route and provide a potential pulmonary delivery system of rifabutin. Moreover, an antimicrobial susceptibility test was performed on the Mycobacterium species *M. phlei*, showing satisfactory antimicrobial activity for the drug-loaded nanocapsules.

These studies embody the first stage of the development of this formulation, towards its future conversion into an inhalable delivery system that would facilitate its administration and directly reach the deep lung, where the rifabutin-loaded nanostructures would be released.

Chitosan nanocapsules have a potential role as polymeric platform for the development of new therapeutic drug delivery systems with improved biodistribution and increased specificity, sensitivity and reduced pharmacological toxicity.

2. Materials and methods

2.1. Materials

Rifabutin, 98%, ACROS Organics ™ was purchased from Fisher Scientific (Madrid, Spain). Miglyol 812^{R} was acquired from Cremer Oleo (Hamburg, Germany), polyethylene glycol stearate 40 (PEG-st 40) was from Croda Chemicals Europe Ltd. (Snaith, United Kingdom), and sodium glycocholate (SGC) was obtained from Dextra Laboratories Ltd. (Reading, United Kingdom). Chitosan HCl (deacetylation degree of 85%, Molecular weight: 30–200 kDa) was purchased from Heppe Medical Chitosan GmbH (Saale, Germany). Lung surfactant (Curosurf®) was obtained from Angelini Pharmacêutica, Lda. (Portugal). SnakeSkin™ Dialysis Tubing 3.5 K MWCO was from Fischer scientific (MO, USA). MTT Formazan, 1-(4,5-Dimethylthiazol-2-yl)−3,5-diphenylformazan, thiazolyl blue formazan, Cation-Adjusted Mueller-Hinton Broth, resazurin and lecithin (Epikuron 145 V) were acquired from Sigma-Aldrich (Madrid, Spain). A549 and Raw 264.7 cell lines and *Mycobacterium phlei* were obtained from ATCC (Manassas, USA). Dulbecco's Modified Eagle Medium (DMEM), Fetal Bovine Serum (FBS), Trypsin-EDTA (0,05%), DiD (1,1′-Dioctadecyl-3,3,3′,3′-Tetramethylindocarbocyanine Perchlorate) and Fluoromount were from Gibco (ThermoFisher Scientific, Madrid, Spain). Triton X-100 (molecular biology grade) was purchased to Scharlab S.L. laboratories (Barcelona, Spain). 4′,6-diamino-2-phenylindole (DAPI) was acquired from Emp-Biotech (Berlin, Germany) and Neutral Buffered Formalin (10% v/v) was bought from Bio-Optica (Milan, Italy). Acetone, ethanol and all other chemicals were of HPLC grade or higher.

2.2. Preparation of the nanocapsules

Blank and rifabutin-loaded chitosan nanocapsules were prepared by a solvent displacement method which was previously developed by our group (Grenha, 2012; Robla et al., 2021). For one-step preparation, in one formulation the oily phase consisted of 6 μl of Miglyol 812, 0.3 ml of PEG-stearate 40 (5.333 mg/ml), and 2 μl of sodium glycocholate (250

mg/ml) as surfactants in a final volume of 0.5 ml of ethanol or acetone. The oily phase of the second formulation contained 6 μl of Miglyol 812 oil and 25 μl of lecithin (100 mg/ml) and 2 μl of sodium glycocholate (250 mg/ml) as surfactants in a final volume of 0.5 ml of ethanol or acetone. The drug rifabutin was dissolved in the oil phase in different concentrations to yield 1, 2, 5, 7 and 10% theoretical loadings. In both cases, the organic phase was poured over 1 ml of chitosan solution (0.5 mg/ml) and was kept under continuous stirring at 400 rpm for 1 h. Then, the organic solvent was removed under vacuum using rotary evaporation (R-300, Büchi, Switzerland) for 5 min at 150 rpm, 37 °C, and 40 mbar to end up with 1 ml final volume. After that, the nanocapsules were isolated by centrifugation (Eppendorf 5430R™, Eppendorf, Hamburg) for 30 min at 4 °C and 20.000 xg and resuspended with 1 ml MilliQ water.

For the two-step preparation method, first a lipid nanoemulsion was formed without a polymer coating, using the same preparation technique as one-step preparation for nanocapsules, and ultrapure water as aqueous phase without chitosan. Thereafter, this lipid nanoemulsion was post-coated by adding a chitosan solution under stirring. Finally, the resulting nanocapsules were isolated by centrifugation (30 min, 4 °C, 20.000 xg, Eppendorf 5430R™, Eppendorf, Hamburg) and are resuspended in 1 ml of ultrapure water.

To explore the possibility of formulating the nanocapsules as dry powder inhalers, the process yields of the lyophilized final product of the nanocapsules were calculated. Blank (without drug) and rifabutin-loaded chitosan nanocapsules were centrifuged for 30 min at 4 °C and 20.000 xg (Eppendorf 5430R™, Eppendorf, Hamburg) and the nanocapsules were freeze-dried for 48 h (from −80 °C to 20 °C by gradually increasing the temperature) using Scanvac Coolsafe 100–9 apparatus (LaboGeneApS, Lynge, Denmark) including mannitol in a ratio of 80/20 (w/w). Subsequently, the nanocapsules (NCs) process yield was calculated by gravimetry using the formula below:

$$\text{P.Y.}(\%) = \frac{\text{NCs weight}}{\text{Total solids } [\text{CS} + \text{Surfactants} + \text{Miglyol} + \text{mannitol}]\text{weight}} \times 100$$

2.3. Physicochemical characterization of the nanocapsules

The size, polydispersity index (PDI), and zeta potential (ZP) of the prepared nanocapsules were measured using a Zetasizer Nano-S (Malvern Instruments; Malvern, UK) at 25 °C. The nanocapsules were diluted 1:20 in ultrapure water (MilliQ^R, Merck, NJ, USA) or cell culture medium (DMEM) before the measurement and the analysis were performed. Analysis was performed at 25 °C with a detection angle of 173° in ultrapure water ($n = 9$).

2.4. Determination of rifabutin association

The encapsulation efficiency (EE%) of rifabutin was determined by quantifying the difference in absorbance of the total amount of the drug and the free drug that is present in the supernatant after centrifugation. For this, centrifugation was carried out as described in Section 2.2 (30 min, 4 °C and 20.000 xg, Eppendorf 5430R™, Eppendorf, Hamburg). The concentration of free rifabutin in the supernatant was measured by UV spectrophotometry (V-730 UV–visible Spectrophotometer, Jasco Deutschland) at 237 nm. A calibration curve for the UV spectrophotometer was obtained using the following concentrations of rifabutin: 0, 2, 4, 6, 8, 10, 12, 15, 17, 20, 23 and 25 μg/ml. The medium for this calibration curve was composed by the supernatant of the blank (non-loaded) nanocapsules diluted in ethanol prior analysis (50:75 v/v); (ethanol: supernatant of blank nanocapsules). This calibration curve has been validated showing adequate accuracy and precision for the concentration range used.

$$\text{EE}\% = \frac{(\text{total drug added} - \text{free non entrapped drug})}{\text{the total drug added})} \text{ X } 100$$

2.5. Morphological characterization

The surface morphology of the nanocapsules was studied using Field Emission Gun Scanning Electron Microscopy (FESEM) and Scanning Transmission Electron Microscopy (STEM) (FESEM Ultra Plus, ZEISS, Germany). Briefly, 10 μl of the 1:100 diluted sample was mixed with 10 μl of 2% phosphotungstic acid. Then, 1 μl of this solution was placed on the bright copper-colored area of the round grid and left until dry. After that, it was washed with water and the grid was left to dry in a desiccator chamber for at least 24 h and then the analysis was performed.

2.6. Stability of the nanocapsules

Physicochemical characteristics of the blank (without drug) and rifabutin-loaded nanocapsules with both formulas were monitored over time. Specifically, the size, PDI, and zeta potential were measured after 1, 7, 14, 21, and 30 days at storage conditions (4 °C) using a Zetasizer Nano-S (Malvern Instruments; Malvern, UK) at 25 °C. The nanocapsules were diluted 1:20 in ultrapure water (MiliQ, Merck, NJ, USA) before the measurement and the analysis was performed as described previously (Section 2.3).

The stability of formulations in supplemented and non-supplemented cellular medium was also investigated. For the study in cellular medium, the suspension of the nanocapsules was diluted 1:20 in DMEM supplemented (10% Fetal Bovine Serum and 1% Penicillin/Streptomycin) and non-supplemented. Then the formulations were mixed under gentle magnetic stirring (300 rpm). At different times (0.25, 1, 2 and 4 h), individual samples were withdrawn and were characterized in terms of mean particle diameter and particle size distribution as described in Section 2.3. This experiment was done in triplicate.

2.7. Release of rifabutin from the nanocapsules

The in-vitro release of rifabutin from the nanocapsules was studied using simulated lung medium, consisting of 10 mM isotonic phosphate buffer saline (PBS) pH 7.4 and 0.1% (v/v) lung surfactant (Curosurf®). 2 ml of the prepared nanocapsules were placed in a dialysis membrane (SnakeSkine dialysis tubing, 3.5 K MECO) and then were added to 50 ml of the dissolution medium on a hotplate under magnetic stirring (37 °C, 300 rpm). After that, 1 ml was withdrawn at 0, 1, 3, 5, 8, 12, and 24 h and replaced with fresh medium to maintain sink conditions. Finally, the amount of rifabutin contained in the dissolution medium at the scheduled time intervals was subsequently analyzed using the UV spectrophotometer at 237 nm wavelength. A calibration curve on the UV spectrophotometer was obtained using 12 concentrations between the range of 0 and 30 μg/mL), utilizing acetonitrile:lung simulated medium: supernatant of blank chitosan nanocapsules (ratio 60:20:20 v/v) as dissolution medium.

2.8. In vitro evaluation in A549 and raw 264.7 cell lines

The A549 and Raw 264.7 cell lines were grown in 10 mL DMEM supplemented with 200 mM L-Glutamine and 10% (v/v) FBS medium, in a humidified incubator (MEMMERT INE 400, Memmert, Germany) with 5% CO_2/95% atmospheric air at 37 °C.

2.8.1. Viability studies

This study was carried out using the 3-(4,5-Dimethylthiazol-2-yl)−2,5-Diphenyltetrazolium Bromide (MTT) assay (Lopes et al., 2012; Mehanna et al., 2011). One day before the experiment, the cells were seeded into a sterile flat bottom 96 well-plate at a density of 6000

cells/well for the A549 cells, 9000 cells/well for the Raw 264.7 cells and left to reach confluence (24 h). After that, the media was removed and the cells were incubated with increasing concentrations of blank or rifabutin 5% loaded nanocapsules (up to 8.5 mg/ml). As negative control (0% viability), 1% of Triton X was used, whereas, for the positive control (100% viability), the untreated cells were incubated with the optimum culture medium. After 4 h of incubation under standard sterile conditions for cell culture (37 °C and 5% CO_2) the samples were removed, the cells were washed and incubated for another 24 h in medium. After that, 10 μl of MTT (5 mg/ml) was added to each well and the plate was incubated for 2 h. In the next step 0.1 ml of isopropanol with 0.04 N HCl was added in order to dissolve the resulting formazan precipitates and give a homogenous blue solution suitable for measurement. Within an hour, the absorbances of the plates were measured at a wavelength of 570 nm according to manufacturers' instructions.

In addition, an evaluation of in vitro cytotoxicity by Luna II was performed. For that purpose, 60,000 A549 cells/well were seeded in 24-well plates (Falcon, USA) with supplemented cell culture medium, and were incubated to grow until confluence (24 h). Cells were treated as follows: (i) 400 μl of supplemented DMEM (1:10) (positive control), (ii) 10 μl of chitosan nanocapsules in a final volume of 400 μl of medium and (iii) a mixture of 10 μl of 1% (v/v) Triton with 390 μl of culture medium (1:10) (negative control). After 4 h of incubation, cells were washed three times with PBS (pH: 7.4) and detached with trypsin. Medium was added to each well and cells were collected and centrifuged for 5 min at 1477 rpm (Eppendorf 5415R Refrigerated Centrifuge, Germany). The pellets were resuspended in 500 μl of PBS (pH 7.4) and 10 μl of the samples were mixed homogeneously with 10 μl of (0.4%, w/v) Trypan Blue stain. Finally, 10 μl of each sample was loaded in a counting chamber to obtain images of the live and dead cells. The viability percentages were obtained by automated counting ($n = 3$). Mean viability values were calculated and expressed as a percentage of live cells (%).

2.8.2. Study of intracellular uptake

For this study, the fluorescent dye DiD (1,1′-Dioctadecyl-3,3,3′,3′-Tetramethylindocarbocyanine Perchlorate) was used to label the nanocapsules. A volume of 6 μl of an ethanolic DiD solution (2.5 mg/ml) was added to the oily phase prior to the nanocapsules preparation. The labeled nanocapsules were characterized as described above, to confirm that their main physicochemical properties remained unaltered and that the dye was stably associated. DiD encapsulation efficiency was determined by quantifying the amount of free dye after isolation of the nanocapsules by fluorescence spectroscopy in a multilabel plate reader (λ_{ex}: 640 nm, λ_{em}: 675 nm).

For the cell internalization study, 60,000 A549 cells/well were seeded on 24-well plates using surface-treated coverslips (Poly-L-Lysine Cellware 12 mm, Corning BioCoat) and were incubated for 24 h until confluence. Then, the culture medium was substituted by (i) 400 μl of supplemented DMEM (control) and (ii) 10 μl/well of DiD-loaded NCs until a final volume of 400 μl of DMEM. Cells were incubated for 4 h and washed three times with PBS (pH 7.4). Cells were fixed by 10% (v/v) neutral buffered formalin for 15 min and washed three times again. Cell nuclei were labeled by adding 200 μl of a 1:1000 (v/v) of DAPI solution. After washing, the coverslips were mounted on the slides using Fluoromount® (Thermo Fisher Scientific, Spain). Samples were observed by confocal laser scanning microscopy (CLSM) (Leica TCS SP5 X, Germany). The fluorescent emissions from DiD ($\lambda_{Ex/Em} = 640/675$ nm) and DAPI ($\lambda_{Ex/Em} = 405/$ 414–440 nm) were captured and the images were colored with red for DiD and blue for DAPI using the LAS X Life Science Software (Leica Microsystems).

To quantify the degree of internalization by A549 and Raw 264.7 cells, the fluorescence-activated cell sorting technique was employed (BD FACSCalibur, BD Biosciences, CA). The cells were treated as above in 24-well plates and after 4 h were detached and isolated by centrifugation (Eppendorf 5415R Refrigerated Centrifuge, Germany) for 5 min at 1477 rpm and 22 °C. The supernatant was removed, and the pellet was resuspended in 500 μl of PBS (pH 7.4) supplemented with 10% FBS. A minimum of 10,000 events were counted at 635 nm using a BP 660/13 filter for DiD, with the forward scatter detector (FSC-A).

2.9. Antimicrobial susceptibility test with Mycobacterium phlei

The antibacterial activity of the rifabutin nanocapsules was evaluated on the rapidly growing mycobacteria *Mycobacterium phlei*, using a resazurin-CAMBH based broth microdilution assay according to EUCAST guidelines (Committee et al., 2003) and CSLI guidelines (Woods, 2011) with slight modifications. This method is rapid and objective, and the minimum inhibitory concentration (MIC) is easily detectable because resazurin (blue) is converted into resorufin (pink fluorescence) in the presence of viable bacteria.

Briefly, nanocapsules containing rifabutin stocks were diluted in 2X Cation-Adjusted Mueller-Hinton Broth (CaMHB) to a final antibiotic concentration of 32 mg/L. Since the susceptibility range of *Mycobacterium* species (Schön and Chryssanthou, 2017; Li et al., 2017) to rifabutin is ≤0.25–16 mg/L and that the CSLI recommended critical cut-off point for *Mycobacterium tuberculosis* (Pfyffer et al., 1999; Farhat et al., 2019), the highest concentration of antibiotic tested was 16 mg/L. Two-fold serial dilutions were performed on 96-well polystyrene plates starting from a 32 mg/L concentration corresponding to rifabutin encapsulated in chitosan nanocapsules (PEG- stearate vs. lecithin as surfactant), using a multichannel pipette. A bacterial suspension in (CaMHB) containing 1.5×10^8 CFU/mL was diluted to a concentration of 10^6 CFU/mL. Then, 100 μl of the adjusted OD_{600} bacterial suspension was added to all wells resulting in approx. 5×10^5 CFU/mL, except for the sterility control wells, and some peripheral wells, which were filled with sterile distilled water, to prevent desiccation during incubation time. For the determination of efficacy, the following controls were used: (i) growth control (wells without treatment) (ii) sterility control (CaMHB), (iii) positive control of the inhibitory effect (free rifabutin in solution) and as well as (iv) empty nanocapsules to account for the possible effects of nanocapsules on bacterial growth.

After a 24 h incubation period at 37 °C, 20 μl of each well were transferred in triplicate to new 96-well plates containing 100 μl of 2X CaMHB, 60 μl 3x PBS and 20 μl resazurin. Resazurin powder was dissolved in PBS (pH 4) to a final concentration of 0.1 mg/ml. Fluorescence intensity was measured at 560 and 590 nm excitation and monitored using the multi-mode reader FLUOR®star Omega (Biotron Healthcare, India) and MARS data analysis software, after an incubation period of 30 min at 37 °C. The lowest concentration at which color change was observed was considered the minimum inhibitory concentration (MIC) value. In addition, the IC_{50} was calculated using an online tool: "Quest Graph™ IC50 Calculator." AAT Bioquest, Inc.

3. Results and discussion

3.1. Optimization and physicochemical characterization of nanocapsules

Blank and rifabutin-loaded chitosan nanocapsules were prepared by a modified solvent displacement technique. The nanocapsules formulation was optimized through a screening of different surfactants (lecithin and PEG-stearate) and solvents (ethanol and acetone), in combination with different drug loadings (1, 2, 5, 7 and 10% of rifabutin). In all cases, the chitosan nanocapsules consisted of a hydrophobic oily core surrounded by a hydrophilic polymeric coating. As shown in Table 1, the nanocapsules with both surfactants were monodispersed with a size range between 130 and 260 nm and, as expected, they exhibited an increase in particle size as the amount/percentage of the loaded rifabutin increased (Gradauer et al., 2012).

In addition, for the design of the nanocapsules, it is important to consider the mesh spacing of the pulmonary environment that would determine the size of cut-off, whereas nanoparticles larger than the mesh size in mucus cannot transport through the physical and biological

Table 1
Physicochemical characterization of chitosan nanocapsules (NCs) with different rifabutin loadings, prepared in one-step, using (A) PEG-stearate and (B) lecithin as surfactant and employing ethanol as solvent (mean ± S.D., $n = 9$).

	Rifabutin (%)	Size (nm)	PDI	Zeta potential (mV)	Product yield (%)
PEG-stearate	Blank	212 ± 6	< 0.1	20 ± 1	96.5 ± 0
	1%	194 ± 9		19 ± 3	96.7 ± 0
	2%	203 ± 11		24 ± 2	96.4 ± 0
	5%	212 ± 22		19 ± 2	97 ± 0
	7%	250 ± 17		23 ± 1	96.5 ± 0
	10%	256 ± 12		18 ± 1	96.8 ± 1
Lecithin	Blank	136. ± 1	< 0.1	31± 1	82.2 ± 4
	1%	134 ± 10		26 ± 2	81.5 ± 3
	2%	132 ± 6		35 ± 1	83.4 ± 1
	5%	157. ± 10		33 ± 2	81.2 ± 1
	7%	161 ± 7		36 ± 1	83.6 ± 5
	10%	177 ± 9		38 ± 3	80.1 ± 4

barriers and are sterically impeded. By contrast, particulates and pathogens smaller than the mesh pore size could theoretically diffuse through the mucus. In this scenario, the size of our nanocapsules is considered suitable for the aimed delivery route. In addition to particle size, the surface charge of the nanoparticles plays another key role in mucociliary clearance. Mucus is rich in negatively charged groups, so positively charged nanostructures will inevitably become immobilized in the mucus network by electrostatic association, thus presenting a mucoadhesive effect to some extent. Increasing mucoadhesion is an effective way to improve pulmonary drug delivery by prolonging lung retention time. Chitosan has been commonly applied to airway mucosa as a positively charged mucoadhesive material (Garbuzenko et al., 2014; Andrade et al., 2013; Liu et al., 2020; Zhu et al., 2005).

In this manner, the surface charges of the prepared nanocapsules, attributed to the presence of a chitosan coat surrounding the oily core, were positive and high enough to provide the nanostructures with sufficient stability (Gradauer et al., 2012).

In the case of nanocapsules prepared with lecithin, particle size was slightly lower and zeta potential values were higher than those of the formulation with PEG-stearate. This difference between the nanocapsules prepared with different surfactants in terms of size and zeta potential could be due to the steric hindrance provided by PEG-stearate chains and the difference in HLB values of the two surfactants (i.e. HLB 7 for lecithin vs. HLB 9 for PEG-stearate) (Zhu et al., 2005).

Size and zeta potential values were also studied with different solvents. For this, as an alternative to ethanol, acetone was used. The values corresponding to this characterization are shown in **table S1**.

3.2. Association of rifabutin

The results of the encapsulation efficiencies of the chitosan nanocapsules containing PEG stearate and lecithin and the different theoretical drug loadings are shown in Table 2. It can be seen that the drug association gradually increases as the theorical drug load increases up to 5% w/w reaching at this drug content the highest values encapsulation efficiencies for both formulations (50.7% ± 6.1 for PEG-stearate and 45.8% ± 2.6 for lecithin, respectively). (Dora et al., 2010; Gooneh-Farahani et al., 2020). Above this threshold, a decrease in the encapsulation efficiencies was observed, which may be due to a saturation of the association process (Gooneh-Farahani et al., 2020).

The encapsulation efficiencies of the corresponding nanoemulsions

Table 2
Encapsulation efficacies (EE%) of rifabutin-loaded chitosan nanocapsules (NCs) prepared using either PEG-stearate or lecithin as surfactants, ethanol or acetone as solvent, and the one-step preparation vs. post-coating preparation method (mean ± S.D., $n = 3$).

	Rifabutin (%)	EE%		
		One-step preparation With ethanol	Post-coating With acetone	With ethanol
PEG-stearate	1%	35.2 ± 5.2	43 ± 8.1	40 ± 4.4
	2%	41.4 ± 4.8	52 ± 6.2	53 ± 4.5
	5%	50.7 ± 6.1	64± 5.2	61 ± 2.5
Lecithin	1%	25.2 ± 2.3	38. ± 12.4	35 ± 9.1
	2%	37.5 ± 12.4	53 ± 7.8	51 ± 8.3
	5%	45.8 ± 2.6	61 ± 6.1	58 ± 5.4

are disclosed in **table S2** (Supplementary material). In order to increase the loading of rifabutin in the nanocapsules, two additional strategies were investigated. First, the solvent, which was initially ethanol, was replaced with acetone to see if the encapsulation efficiency would thus be increased. The second consisted in a two-step preparation process, by the post-coating of the corresponding nanoemulsions (with ethanol as solvent) with chitosan.

When replacing the solvent with acetone, as it can be seen see in Table 2 it was observed that the percentage of rifabutin encapsulation increased for the rifabutin-loaded formulations for both types of nanocapsules up to 5% w/w, reaching at this drug content the highest encapsulation efficiencies values for both formulations (64% ± 5.2 for PEG-stearate and 61% ± 6.1 for lecithin, respectively).

In addition, when the original one-step preparation method was compared with a two-step process (i.e. post-coating of a pre-formed nanoemulsion as described in Section 2.2), using ethanol as solvent in both cases, the two-step process did not improve remarkably the encapsulation efficiency, obtaining encapsulation efficiency values similar to the formulations with acetone as solvent.

3.3. Morphological characterization

Different microscopy techniques were used to characterize and evaluate the morphology of the nanocapsules. FESEM and STEM microscopy images (Fig. 1) revealed a homogeneous population of particles with round-shaped structures, (Mehanna et al., 2011; Andrade et al., 2013). The average particle diameter was about 200 nm which perfectly

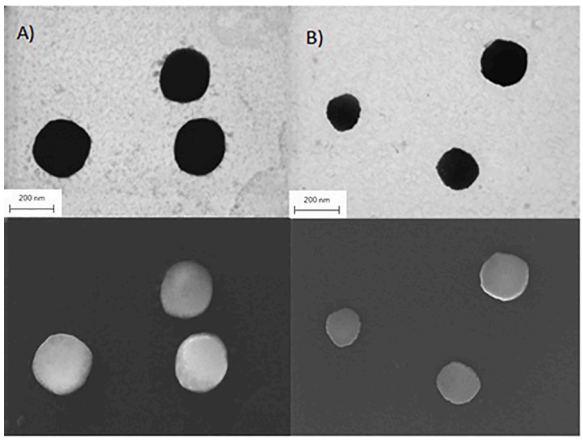

Fig. 1. Representative electron micrographs of nanocapsules prepared in one-step with (A) PEG-stearate and (B) with lecithin as surfactant using ethanol as solvent. Above: images obtained by TEM. Below: images obtained by SEM. Bars represent 200 nm in both cases.

correlated with the average particle size that was obtained using the DLS technique (Tuoriniemi et al., 2014). No remarkable differences were observed between the rifabutin loaded and the blank nanocapsules.

3.4. Stability of nanocapsules

The storage stability of blank (PEG-stearate or lecithin) and rifabutin-loaded nanocapsules (1, 2, 5, and 7% w/w) was determined in aqueous suspensions at 4ºC for 30 days. All formulations were stable after one month with respect to size, PDI and zeta potential up to theoretical rifabutin loadings of 5% (**Figure S1 and S2).** On the other hand, nanocapsules loaded with 10% rifabutin nanocapsules were not stable as both the size and the PDI increased with time, probably due to the nanosystems saturation (Masarudin et al., 2015). Taking into account the above results, the formulations with 5% w/w theoretical drug loading were selected for further characterization and efficacy evaluation (Fig. 2).

In terms of stability in DMEM (cellular medium), an increase of particle size was observed with time when PEG-stearate nanocapsules were incubated in supplemented DMEM, achieving 700 nm for the PEG-stearate nanocapsules at 4 h. However, particles size was practically constant, below 200 nm for the lecithin nanocapsules. When nanocapsules were incubated with DMEM without supplementation, the sizes remained stable with time for both formulations (Fig. 3). As for the count rate of nanocapsules, these remained stable for 4 h in both supplemented and non-supplemented medium, indicating negligible particles aggregation or precipitation (**Figure S3**).

Overall, the nanostructures containing lecithin seem to be more stable than PEG-stearate nanocapsules under the tested conditions. Nevertheless, as indicated by the analysis of the particle count rate, which remained constant during these studies, suggesting, as previously mentioned, the absence of particle aggregation, both formulations were considered to have sufficient stability for the purpose of in vitro cell studies.

3.5. In vitro drug release

The in-vitro release behavior of rifabutin from the nanocapsules was investigated using simulated lung medium (pH = 7.4), whose composition was described in Section 2.7.

As shown in Fig. 4**,** the nanocapsules prepared with either PEG-sterate or lecithin showed an initial fast release phase of rifabutin, reaching approximately 30% of drug release for both nanoformulations at 5 h. After 12 h, differences between the release patterns could be observed, since the release rate slowed down for the lecithin capsules while the PEG-stearate containing nanocapsules showed faster rifabutin release. Overall, after 24 h the amount of the released rifabutin was about 62% and 41%, from the formulations containing PEG-stearate lecithin, respectively. If we compare these data with those obtained from the nanoemulsions, we can conclude that the nanocapsules provide a more sustained release pattern of rifabutin with respect to nanoemulsion independently of the surfactant used in the core nanostructures. These differences could be attributed to the presence of the chitosan shell around the drug containing oily core, that can modulate the release kinetics (Altaani et al., 2019).

3.6. In-vitro cell viability study in A549 and raw 264.7 cells

As cationic nanoparticles generally have superior electrostatic interaction with the negatively charged membrane surface, their toxicity might be considered as a critical parameter and determined accordingly. To examine the biocompatibility of both blank and rifabutin-loaded chitosan nanocapsules on the lung cells, first we performed an evaluation by Luna II in A549 lung cells (data shown in **Figure S4**). The viability percentages were obtained by automated counting and viability values were calculated and expressed as percentage of live cells (%). When the cells were incubated with the nanocapsules, they presented a viability higher than 85% in all cases. In view of the obtained results, we further investigated the compatibility of the nanosystems by an in vitro MTT that was performed in lung derived A549 lung cells and Raw 264.7 macrophages.

As shown in Fig. 5**A,** after 4 h of incubation of the rifabutin-loaded nanocapsules with the A549 lung epithelial cells, the viability of the cells was maintained above 90%, up to a concentration of 4.25 mg/ml, regardless of the surfactant type or drug loading.

Above this concentration, a slight decrease in the viability of the cells was observed, which was more pronounced in the case of drug loaded nanocapsules. Moreover, as it can be seen in Fig. 5**B**, similar results were obtained after 4 h of incubation of rifabutin-loaded nanocapsules with the Raw 264.7 macrophage cell line. High viability is maintained for all formulations up to 4.25 mg/ml concentrations, after which a slight descent is observed for all formulations. This decrease is more pronounced in the case of rifabutin-loaded nanocapsules with lecithin.

Overall, the results of these studies indicated that the drug and the drug-loaded nanocapsules formulations were well tolerated by the cells and safe to be used for pulmonary delivery.

3.7. Study of intracellular uptake

It is well known that chitosan promotes the transcellular and paracellular penetration of nanosystems, which is related to its mucoadhesive properties. Therefore, chitosan nanocapsules were expected to interact efficiently with both cell lines used in this study. The internalization was observed by CLSM using DAPI (blue channel) to label the cell nuclei and Did (red channel) to label the nanocapsules, as previously described.

The representative images shown in Figs. 6 **and** 7 verify the internalization of the nanosystems, indicating that both nanosystems were efficiently uptaken by the A549 and Raw 264.7 cell lines, where they are mostly localized in the cytoplasmatic region.

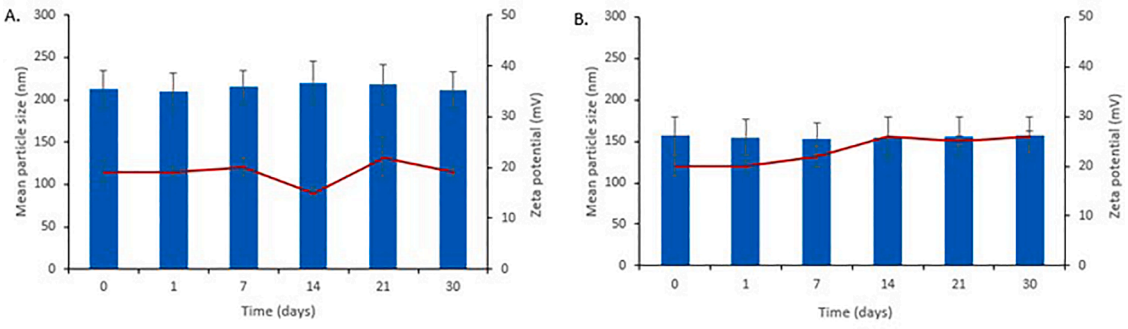

Fig. 2. Evolution of particle size (bars) and zeta potential (continuous line) of 5% rifabutin-loaded nanocapsules prepared in one-step, containing with (A) PEG-stearate and with (B) lecithin as surfactant at 4 °C using ethanol as solvent (mean ± S.D., $n = 3$).

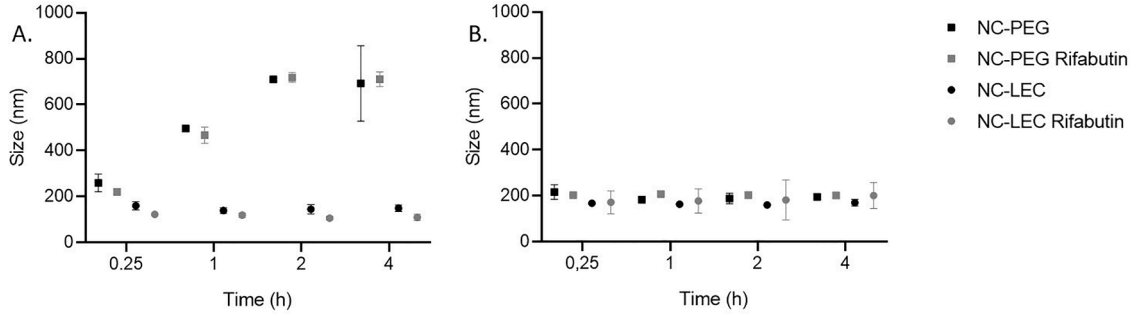

Fig. 3. Stability of chitosan nanocapsules prepared in one-step and using ethanol as solvent in DMEM (A) supplemented and (B) without supplementation. Black: blank nanocapsules; Grey: rifabutin-loaded nanocapsules (mean ± S.D., $n = 3$).

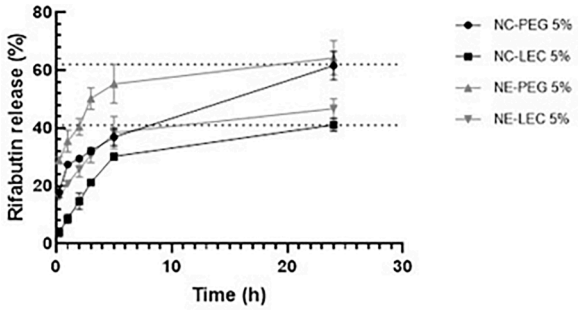

Fig. 4. Cumulative release (%) of rifabutin from PEG-stearate nanocapsules and nanoemulsions (NC-PEG/NE-PEG) prepared in one-step and lecithin nanocapsules and nanoemulsions (NC-LEC/NE-LEC) in simulated lung medium (PBS, pH 7.4 and 0.1% (v/v) lung surfactant (Curosurf®) (mean ± S.D., $n = 3$).

3.8. Quantification of cellular uptake in A549 and Raw 264.7 cells

To determine the percentage of cells internalized with nanocapsules, a FACS analysis was performed comparing the histogram of control cells with those obtained for the cells treated with the nanocapsules. Fig. 8 showed that, as expected, the control cells were negative to the signal of DiD. When the cells were treated with nanocapsules, the DiD signal appeared as an indication of their internalization.

Therefore, both types of nanosystems were uptaken by almost the total of A549 cells, 98.9% and 99.9% in the case of PEG-stearate and lecithin respectively. In addition, the results of this study were congruent with those obtained with confocal images and they further support that both nanosystems show efficient cellular interaction and internalization in vitro. Similar results were obtained for the Raw 264.7 macrophage cell line (Fig. 9), showing nanocapsules internalization for more than 90% of the cells. However, if we compare the fluorescence intensities, it can be seen that the values corresponding to the lecithin nanocapsules are generally higher than those of PEG-stearate. This might be explained by a greater number of nanocapsules reaching the interior of the cell.

3.9. Antimicrobial susceptibility test in Mycobacterium phlei

The in vitro efficacy of the rifabutin-loaded chitosan nanocapsules was evaluated by monitoring their inhibitory effect on the rapidly-growing Mycobacterium species *M. phlei*, as compared to the effect of non-encapsulated rifabutin. Blank nanocapsules showed no inhibitory effect and upon an overnight incubation, the bacteria showed free growth patterns similar to the untreated wells used as reference. In contrast, Fig. 10 **shows** the average growth of *M. phlei* in presence of different concentrations of nanocapsules with PEG-stearate or lecithin, where complete inhibition was observed for antibiotic concentrations ≥ 0.25 mg/L in both cases. This is in agreement with the susceptibility range of *Mycobacterium* (≤0.25–16 mg/L). Below this concentration, a slight difference could be observed between the two nanocapsules compositions, as indicated by their IC50 value (Table 3). Nanocapsules containing lecithin seem to show a slightly higher inhibitory effect than those containing PEG-stearate. This could be attributed to the differences observed in the previous in vitro release and the cellular interaction of the formulations. As commented above in the previous section, although both formulations showed cellular internalization greater than 90% of the cells, overall, we would obtain higher values for the nanocapsules that contained lecithin as a surfactant. This may be explained by the fact that a greater number of nanocapsules can reach the interior of the cell, which may also explain why the nanocapsules containing lecithin as a surfactant have a slightly higher inhibitory effect than the other formulation with PEG-stearate.

In this study, the IC_{50} value represents the minimum concentration of the antibiotic loaded in the tested nanoparticles necessary to inhibit by

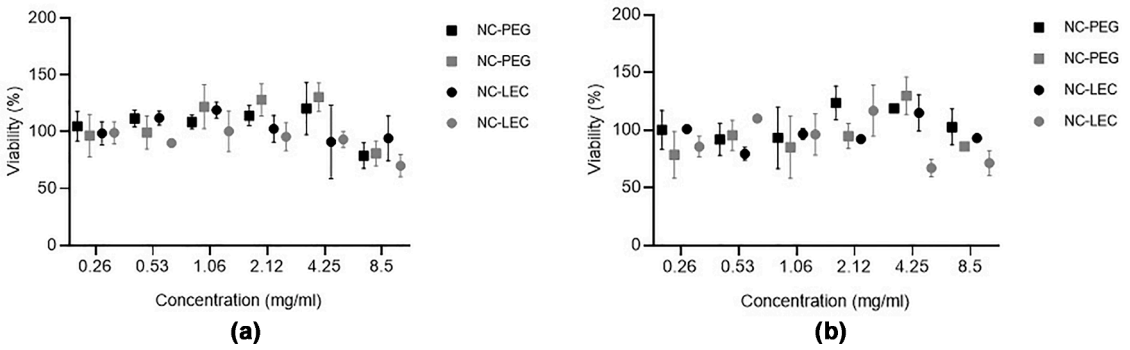

Fig. 5. A: Viability of A549 cells with different concentrations of nanocapsules prepared in one-step after 4 h of incubation. Black: blank nanocapsules with PEG-stearate (NC-PEG) and lecithin (NC-LEC); Grey: rifabutin-loaded nanocapsules. (mean ± S.D, $n = 3$). B: Viability of Raw 264.7 cells incubated with different concentrations of chitosan nanocapsules prepared in one-step after 4 h of incubation. Black: blank; Grey: rifabutin-loaded (mean ± S.D., $n = 3$).

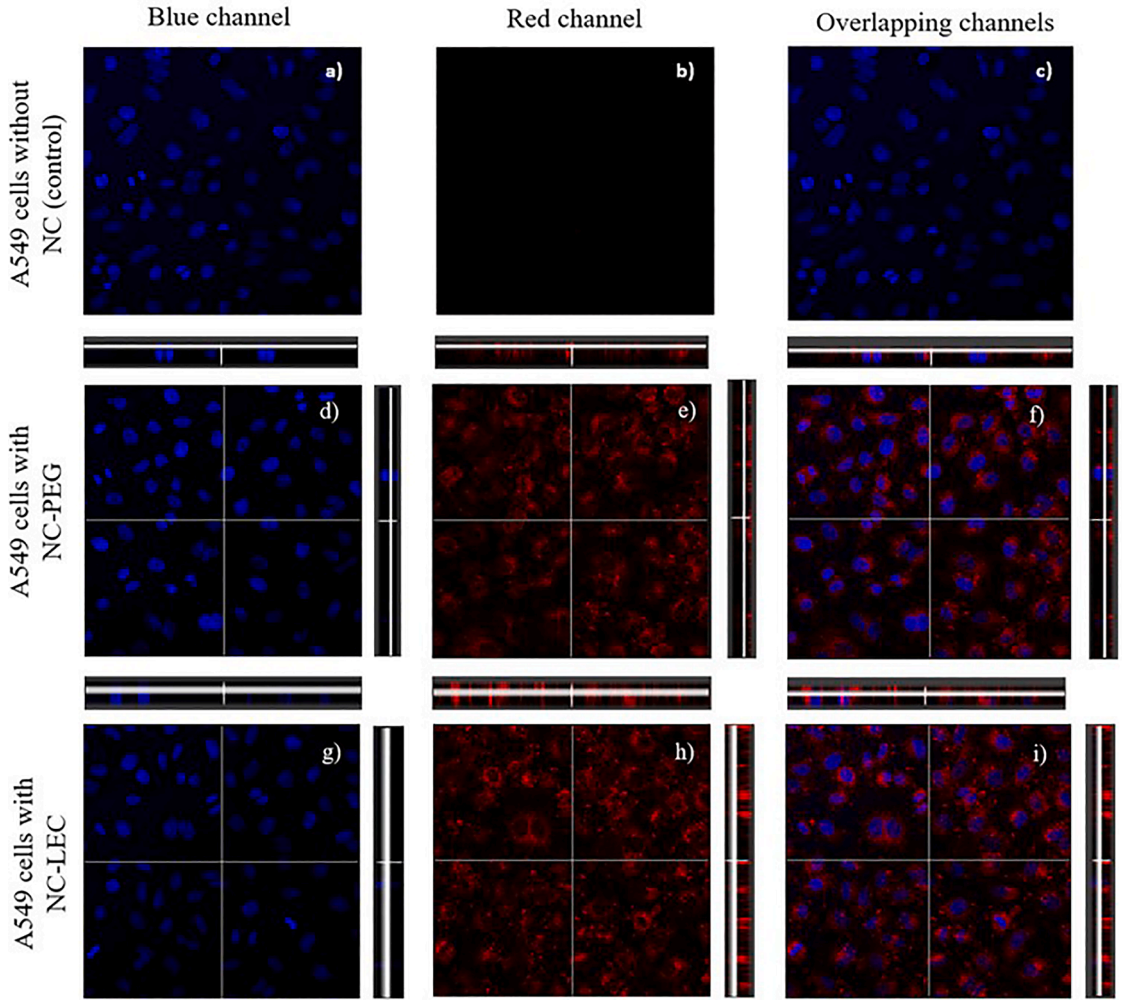

Fig. 6. Confocal microscopy images of A549 cells: control: without nanocapsules (a-c), treated with 10 μl/well of nanocapsules with PEG-stearate (d-f) and nanocapsules with lecithin (g-i), with corresponding z stacks aligned to the right and above. Red channel (DiD): nanocapsules; Blue channel (DAPI): cell nuclei. (For interpretation of the references to color in this figure legend, the reader is referred to the web version of this article.)

50% the *Mycobacterium phlei* growth in vitro. Our results (Table 3 **and Figure S5**) showed an IC_{50} of 0.15 mg/L for nanocapsules with PEG-stearate as surfactant and 0.11 mg/L for nanocapsules with lecithin as surfactant, the latter value corresponding to the IC50 of free rifabutin, indicating adequate release of the antibiotic.

However, despite the differences observed at lower concentrations, we can conclude that both formulations have a minimum inhibitory concentration (MIC) of 0.25 mg/L which, as previously mentioned, is within the susceptibility range of *Mycobacterium* and corresponds to the MIC obtained for our positive control using free rifabutin (Table 3).

Overall, the results obtained in these studies indicate that chitosan nanocapsules can efficiently deliver and release rifabutin and that the released drug displays an inhibitory effect on *Mycobacterium phlei* similar to the free drug. Nevertheless, as previously mentioned, in vitro studies demonstrated an internalization in more than 90% of the cells, and during the first hour we were able to observe, that a large proportion of nanocapsules were localized in the cytoplasmic region. In addition, we obtained a release profile of rifabutin, where our nanocapsules were able to release the drug for at least 24 h. It can be understood from the results that, although the inhibitory effect is similar to that of free rifabutin, the nanocapsules offer additional benefits by allowing a more localized and sustained treatment, reducing the side effects associated to systemic administration of drugs. However, further studies should be carried out in the future to gain more knowledge on the in vivo antibacterial potential of the delivery system. In fact, as previously mentioned, it has recently been demonstrated that chitosan nanostructures may exert anti-quorum sensing activity with particular relevance in the current context of increasing propagation of resistances to antibiotics (Nag et al., 2021).

In addition, it is also necessary to consider the pH value of the formulations developed as well as how the dilutions in different media can affect the chitosan loading and therefore its antibacterial activity. The final pH of the nanocapsules formulations resuspended in water is 4.6, while the pH of the bacterial media is around 6; however, the simulated lung fluid and the cellular media are at pH 7. Chitosan has a pka value around 6.5 and at higher than this, specifically above pH 7 as in simulated lung media or cell media, the bacterial activity decreases. It has been suggested that a positive charge on the NH_3^+ group of the glucosamine monomer at low pH allows interaction with negatively charged microbial cell membranes, leading to agglutination and leakage of intracellular constituent (Fei Liu et al., 2000). Pulmonary disease by *Mycobacterium tuberculosis* is characterized by the formation of granulomas that arise in response to a persistent stimulus. The main function of the granuloma is to localize and confine the infection while concentrating the immune response to a certain area. In these structures, the bacilli are exposed to a variety of stressful conditions, such as hypoxia, acidic pH, and nutrient deprivation (Zs et al., 2021).

Indeed, it was previously reported that granulomas exhibit a more acidic microenvironment (pH 5.8) and to this end, chitosan nanocapsules can offer benefits for delivering antibiotics to acidic

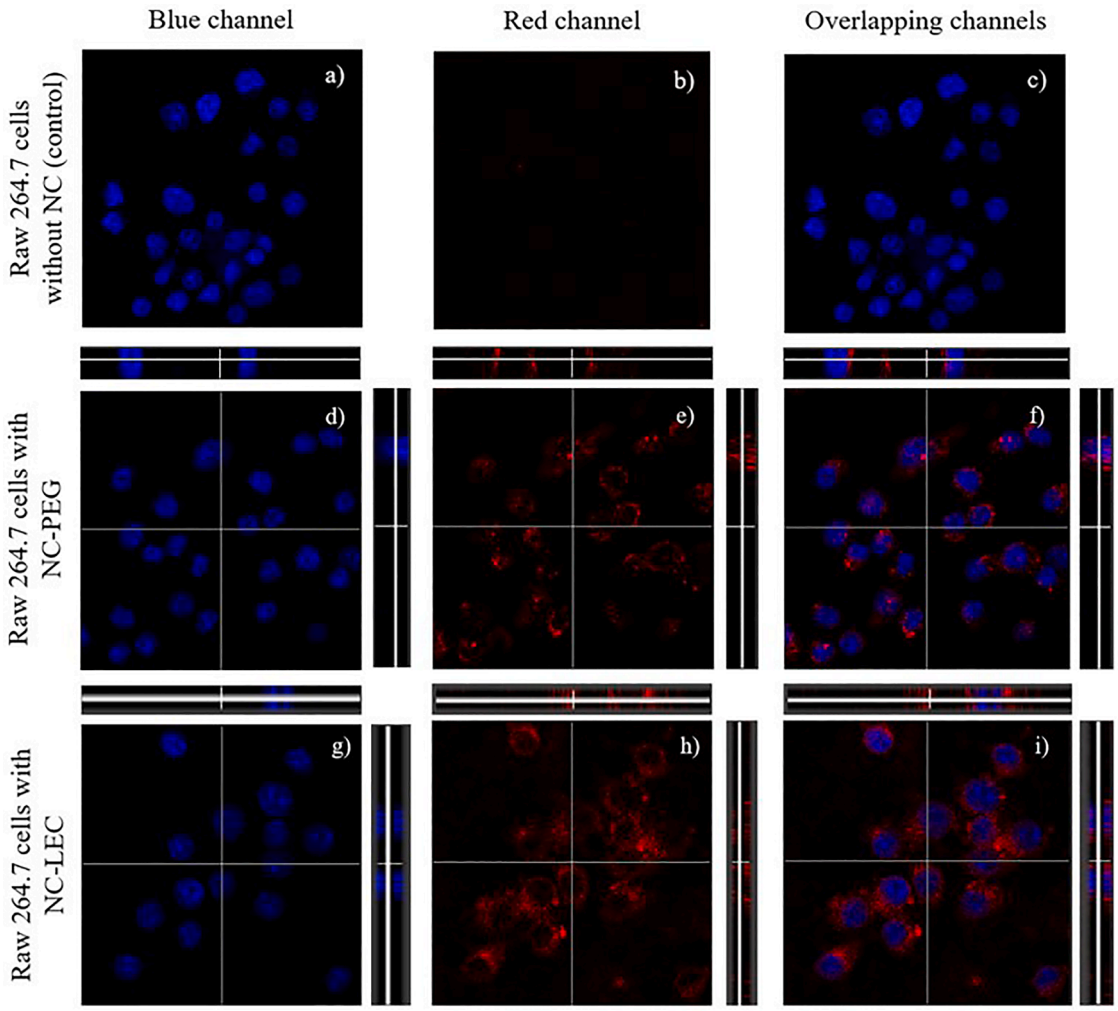

Fig. 7. Confocal microscopy images of Raw 264.7 cells: control: without nanocapsules (a-c), treated with 10 μl/well of nanocapsules with PEG-stearate (d-f) and nanocapsules with lecithin (g-i) with corresponding z stacks aligned to the right and above. Red channel (DiD): nanocapsules; Blue channel (DAPI): cell nuclei. (Z = 5). (For interpretation of the references to color in this figure legend, the reader is referred to the web version of this article.)

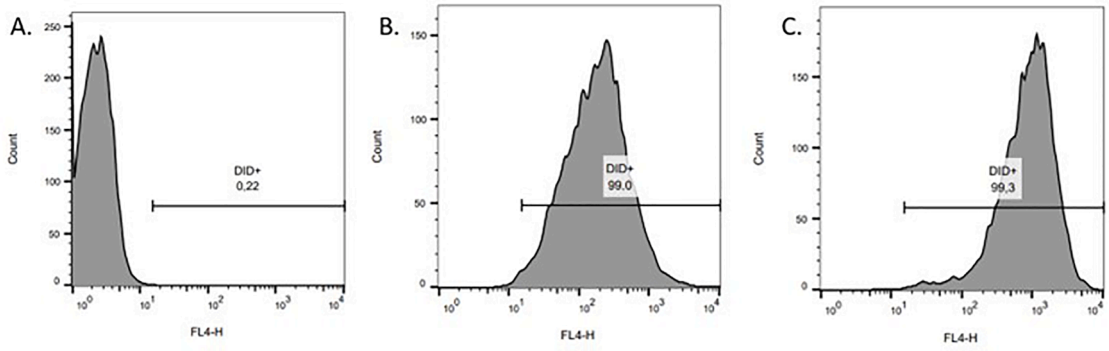

Fig. 8. FACS histograms of A549 cells: (A) control, treated with PEG-stearate nanocapsules (B) and (C) treated with lecithin nanocapsules prepared in one-step.

granulomas tissues with a high local concentration, thus effectively minimizing the adverse effects resulting from drugs (Piccaro et al., 2013).

4. Conclusions

A chitosan-based nanoencapsulated delivery systems were developed for the encapsulation of the antitubercular drug rifabutin. Results show that by the appropriate combination of surfactants and solvents, drug-loaded nanocapsules can be obtained with satisfactory stability and suitable, sustained release patterns. The in vitro cell viability and uptake studies showed efficient internalization of the nanosystems, with main localization in the cytoplasm, while maintaining cellular morphology and integrity. In addition, the antimicrobial susceptibility test confirmed the antibacterial activity of the drug is maintained upon its encapsulation into the nanosystems, indicating that chitosan

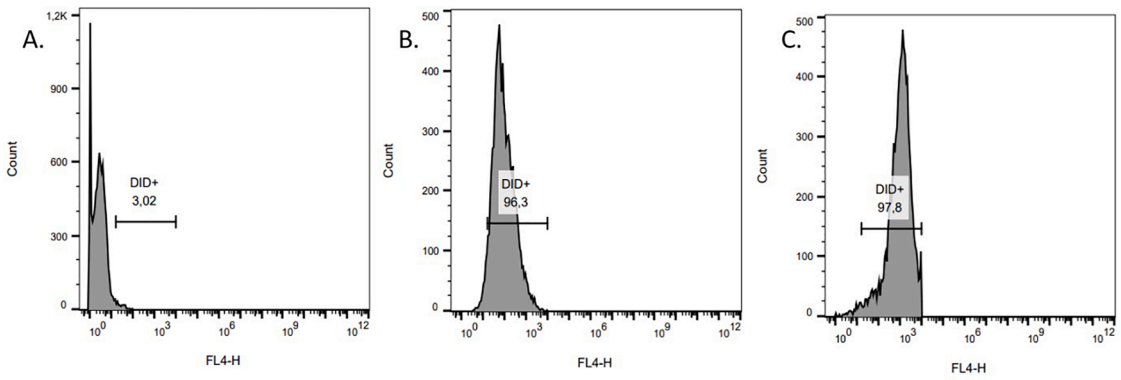

Fig. 9. FACS histograms of RAW 264.7 cells: (A) control, treated with PEG-stearate nanocapsules (B) and treated with lecithin nanocapsules (C) prepared in one-step.

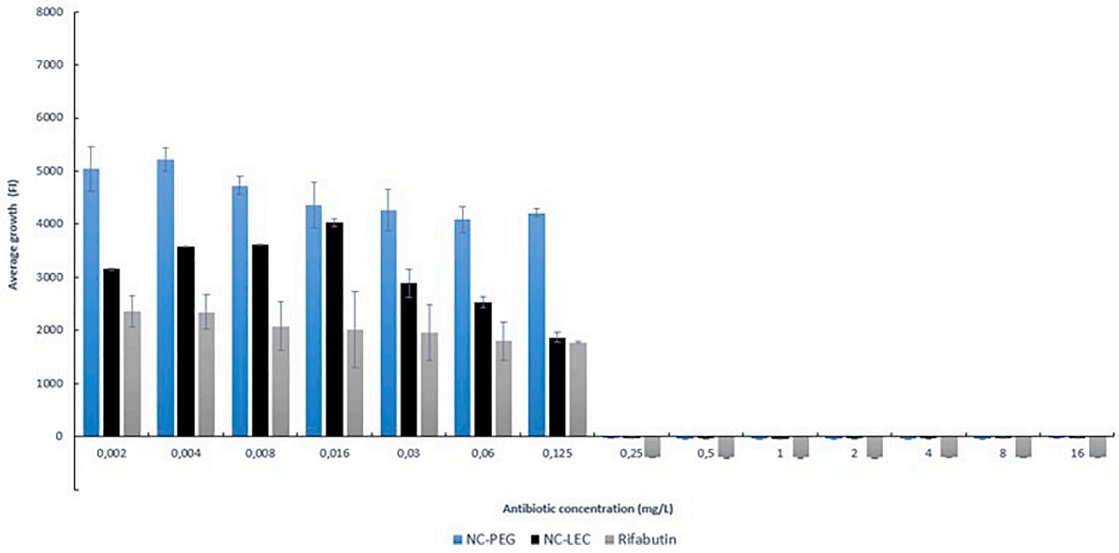

Fig. 10. Average growth of *Mycobacterium phlei* (expressed as fluorescence intensity) in presence of rifabutin-loaded chitosan nanocapsules (NC-PEG or NC-LEC) or free rifabutin in solution. The average value of the blank (sterility control) shown was subtracted from all values. (mean ± S.D, $n = 9$). (For interpretation of the references to color in this figure legend, the reader is referred to the web version of this article.)

Table 3
Minimum inhibitory concentrations (MIC) and half-maximal inhibitory concentrations (IC50) values in mg/L of rifabutin-loaded nanocapsules with PEG-stearate (NC-PEG), lecithin (NC-LEC) and free rifabutin for *Mycobacterium phlei*.

	NC-PEG	NC-LEC	Free rifabutin
MIC (mg/L)	0.25	0.25	0.25
IC50 (mg/L)	0.15	0.11	0.11

nanocapsules can efficiently deliver and release intact rifabutin. Overall, these nanocarriers could be interesting candidates as delivery systems to the lung mucosa for the local pulmonary treatment of infectious diseases.

In order to facilitate the pulmonary administration of the nanocapsules, these can be administered with the aid of a nebulizer or as a dry powder inhaler. For the latter, in future studies rifabutin-loaded chitosan nanocapsules could be incorporated into microparticles by freeze-drying or co-spray drying with mannitol to obtain a dry powder with suitable aerodynamic properties. The ready-to-use pulmonary dry powder systems to be developed could be very promising for inhalable therapy of pulmonary tuberculosis and could be one of the alternatives to be studied in the future.

CRediT authorship contribution statement

Lorena Valverde-Fraga: Formal analysis, Investigation, Methodology, Software, Visualization, Writing – original draft, Writing – review & editing. **Razan Haddad:** Investigation, Writing – original draft. **Nasr Alrabadi:** Writing – original draft. **Sandra Sánchez:** Supervision, Methodology, Writing – review & editing. **Carmen Remuñán-López:** Supervision, Funding acquisition, Validation, Visualization, Writing – review & editing. **Noemi Csaba:** Conceptualization, Funding acquisition, Resources, Project administration, Supervision, Validation, Visualization, Writing – review & editing.

Declaration of Competing Interest

The authors declare no conflict of interest.

Data availability

Data will be made available on request.

Acknowledgments

This work has received financial support from the Xunta de Galicia

(Centro singular de investigación de Galicia, accreditation 2019–2022); Competitive Reference Groups, ED431C 2021/17-FEDER) and Ministerio de Ciencia e Innovación, Gobierno de España (PID2019-107500RB-I00).

Supplementary materials

Supplementary material associated with this article can be found, in the online version, at doi:10.1016/j.ejps.2023.106484.

References

Altaani, B.M., Al-Nimry, S.S., Haddad, R.H., Abu-Dahab, R., 2019. Preparation and characterization of an oral norethindrone sustained release/controlled release nanoparticles formulation based on Chitosan. AAPS PharmSciTech 20 (2).

Andersen, P., Doherty, T.M., Pai, M., Weldingh, K., 2007. The prognosis of latent tuberculosis: can disease be predicted? Trends Mol. Med. 13 (5), 175–182.

Andrade, F., Rafael, D., Videira, M., Ferreira, D., Sosnik, A., Sarmento, B., 2013. Nanotechnology and pulmonary delivery to overcome resistance in infectious diseases. Adv. Drug. Deliv. Rev. 65 (13–14), 1816–1827.

Aranaz, I., Mengibar, M., Harris, R., Panos, I., Miralles, B., Acosta, N., et al., 2012. Functional characterization of Chitin and Chitosan. Curr. Chem. Biol. 3 (2), 203–230.

Baranyai, Z., Soria-Carrera, H., Alleva, M., Millán-Placer, A.C., Lucía, A., Martín-Rapún, R., et al., 2021. Nanotechnology-based targeted drug delivery: an emerging tool to overcome tuberculosis. Adv. Ther. 4 (1), 1 de enero de.

Brainard, D.M., Kassahun, K., Wenning, L.A., Petry, A.S., Liu, C., Lunceford, J., et al., 2011. Lack of a clinically meaningful pharmacokinetic effect of rifabutin on raltegravir: in vitro/in vivo correlation. J. Clin. Pharmacol. 51 (6), 943–950.

Burman, W.J., Gallicano, K.P.C, 2001. Comparative pharmacokinetics and pharmacodynamics of the Ryfamycin Antibacterials. Clin. Pharmacokinet. 40 (5), 327–341.

Clemens, D.L., Lee, B.Y., Xue, M., Thomas, C.R., Meng, H., Ferris, D., et al., 2012. Targeted intracellular delivery of antituberculosis drugs to Mycobacterium tuberculosis-infected macrophages via functionalized mesoporous silica nanoparticles. Antimicrob. Agents Chemother. 56 (5), 2535–2545.

Committee, E., Testing, S., Microbiology, C., Escmid, I.D., 2003. Determination of minimum inhibitory concentrations (MICs) of antibacterial agents by broth dilution. Clin. Microbiol. Infect. 9 (8) ix-xv.

Costa, E.M., Silva, S., Pina, C., Tavaria, F.K., Pintado, M., 2014. Antimicrobial effect of chitosan against periodontal pathogens biofilms. SOJ Microbiol. Infect. Dis. 2 (1), 1–6, 1 de Enero de.

Dodane, V., Vilivalam, V.D., 1998. Pharmaceutical applications of chitosan. Pharm. Sci. Technol. Today 1 (6), 246–253.

Dora, C.P., Singh, S.K., Kumar, S., Datusalia, A.K., Deep, A., 2010. Development and characterization of nanoparticles of glibenclamide by solvent displacement method. Acta Pol. Pharm. - Drug Res. 67 (3), 283–290.

Farhat, M.R., Sixsmith, J., Calderon, R., Hicks, N.D., Fortune, S.M., Murray, M., 2019. Rifampicin and rifabutin resistance in 1003 Mycobacterium tuberculosis clinical isolates. J. Antimicrob. Chemother. 74 (6), 1477–1483.

Fei Liu X., Lin Guan Y., Zhi Yang D., Yao K.D.E. Antibacterial Action of Chitosan and Carboxymethylated Chitosan. 2000.

Garbuzenko, O.B., Mainelis, G., Taratula, O., Minko, T., 2014. Inhalation treatment of lung cancer: the influence of composition, size and shape of nanocarriers on their lung accumulation and retention. Cancer Biol. Med. 11 (1), 44–55.

Gaspar, D.P., Faria, V., Gonçalves, L.M.D., Taboada, P., Remuñán-López, C., Almeida, A. J., 2016. Rifabutin-loaded solid lipid nanoparticles for inhaled antitubercular therapy: physicochemical and in vitro studies. Int. J. Pharm. 497 (1–2), 199–209.

Gaspar, D.P., Gaspar, M.M., Eleutério, C.V., Grenha, A., Blanco, M., Gonçalves, L.M.D., et al., 2017. Microencapsulated solid lipid nanoparticles as a hybrid platform for pulmonary antibiotic delivery. Mol. Pharm. 14 (9), 2977–2990.

Gooneh-Farahani, S., Naghib, S.M., Naimi-Jamal, M.R., 2020. A novel and inexpensive method based on modified ionic gelation for pH-responsive controlled drug release of homogeneously distributed chitosan nanoparticles with a high encapsulation efficiency. Fibers Polym. 21 (9), 1917–1926.

Gradauer, K., Vonach, C., Leitinger, G., Kolb, D., Fröhlich, E., Roblegg, E., et al., 2012. Chemical coupling of thiolated chitosan to preformed liposomes improves mucoadhesive properties. Int. J. Nanomed. 7, 2523–2534.

Grenha, A., Grainger, C.I., Dailey, L.A., Seijo, B., Martin, G.P., Remuñán-López, C., et al., 2007. Chitosan nanoparticles are compatible with respiratory epithelial cells in vitro. Eur. J. Pharm. Sci. 31 (2), 73–84.

Grenha, A., 2012. Chitosan nanoparticles: a survey of preparation methods. J. Drug Target 20 (4), 291–300.

Huang, Y.C., Vieira, A., Yeh, M.K., Chiang, C.H., 2007. Pulmonary anti-inflammatory effects of chitosan microparticles containing betamethasone. J. Bioact. Compat. Polym. 22 (1), 30–41.

Illum, L., 1998. Chitosan and its use as a pharmaceutical excipient. Pharm. Res. 9, 1326–1331.

Jeon, S.J., Oh, M., Yeo, W.S., Galvão, K.N., Jeong, K.C., 2014. Underlying mechanism of antimicrobial activity of Chitosan microparticles and implications for the treatment of infectious diseases. PLoS ONE 9 (3), 92723.

Kaur, M., Garg, T., Narang, R.K., 2016. A review of emerging trends in the treatment of tuberculosis. Artif Cells. Nanomed. Biotechnol. 44 (2), 478–484.

Kean, T., Thanou, M., 2010. Biodegradation, biodistribution and toxicity of chitosan. Adv. Drug. Deliv. Rev. 62 (1), 3–11.

Khan, F., Pham, D.T.N., Oloketuyi, S.F., Manivasagan, P., Oh, J., Kim, Y.M., 2020. Chitosan and their derivatives: antibiofilm drugs against pathogenic bacteria. Colloids Surf. B Biointerfaces 185 (November 2019), 110627.

Li, G., Pang, H., Guo, Q., Huang, M., Tan, Y., Li, C., et al., 2017. Antimicrobial susceptibility and MIC distribution of 41 drugs against clinical isolates from China and reference strains of nontuberculous mycobacteria. Int. J. Antimicrob. Agents 49 (3), 364–374.

Liu, H., Du, Y., Wang, X., Sun, L., 2004. Chitosan kills bacteria through cell membrane damage. Int. J. Food Microbiol. 95 (2), 147–155.

Liu, Q., Guan, J., Qin, L., Zhang, X., Mao, S., 2020. Physicochemical properties affecting the fate of nanoparticles in pulmonary drug delivery. Drug Discov. Today 25 (1), 150–159.

Lopes, R., Eleutério, C.V., Gonalves, L.M.D., Cruz, M.E.M., Almeida, A.J., 2012. Lipid nanoparticles containing oryzalin for the treatment of leishmaniasis. Eur. J. Pharm. Sci. 45 (4), 442–450.

Masarudin, M.J., Cutts, S.M., Evison, B.J., Phillips, D.R., Pigram, P.J., 2015. Factors determining the stability, size distribution, and cellular accumulation of small, monodisperse chitosan nanoparticles as candidate vectors for anticancer drug delivery: application to the passive encapsulation of [14C]-doxorubicin. Nanotechnol. Sci. Appl. 8, 67–80.

Mehanna, C., Baudouin, C., Brignole-Baudouin, F., 2011. Spectrofluorometry assays for oxidative stress and apoptosis, with cell viability on the same microplates: a multiparametric analysis and quality control. Toxicol. Vitr. 25 (5), 1089–1096.

Nag, M., Lahiri, D., Mukherjee, D., Banerjee, R., Garai, S., Sarkar, T., et al., 2021. Functionalized Chitosan nanomaterials: a jammer for quorum sensing. Polymer 13, 2533. Page30 de julio de 2021;13(15):2533.

Pai, R.V., Jain, R.R., Bannalikar, A.S., Menon, M.D., 2016. Development and evaluation of chitosan microparticles based dry powder inhalation formulations of Rifampicin and Rifabutin. J. Aerosol. Med. Pulm. Drug Deliv. 29 (2), 179–195.

Pandey, R., Ahmad, Z., 2011. Nanomedicine and experimental tuberculosis: facts, flaws, and future. Nanomed. Nanotechnol. Biol. Med. 7 (3), 259–272.

Pandey, R., Khuller, G.K., 2005. Solid lipid particle-based inhalable sustained drug delivery system against experimental tuberculosis. Tuberculosis 85 (4), 227–234.

Pfyffer, G.E., Bonato, D.A., Ebrahimzadeh, A., Gross, W., Hotaling, J., Kornblum, J., et al., 1999. Multicenter laboratory validation of susceptibility testing of Mycobacterium tuberculosis against classical second-line and newer antimicrobial drugs by using the radiometric BACTEC 460 technique and the proportion method with solid media. J. Clin. Microbiol. 37 (10), 3179–3186.

Piccaro, G., Giannoni, F., Filippini, P., Mustazzolu, A., Fattorini, L., 2013. Activities of drug combinations against mycobacterium tuberculosis grown in aerobic and hypoxic acidic conditions. Antimicrob. Agents Chemother. 57 (3), 1428–1433 marzo de.

Pinheiro, M., Lucio, M., Lima, J.L.F.C., Reis, S., 2011. Liposomes as drug delivery systems for the treatment of TB: passive & active targeting of liposomes as drug delivery systems for the treatment of TB. Nanomedicine 6 (8), 1413–1428.

Qin, X., Engwer, C., Desai, S., Vila-Sanjurjo, C., Goycoolea, F.M., 2017. An investigation of the interactions between an E. coli bacterial quorum sensing biosensor and chitosan-based nanocapsules. Colloids Surf. B Biointerfaces 149, 358–368, 1 de Enero de.

Rashki, S., Asgarpour, K., Tarrahimofrad, H., Hashemipour, M., Ebrahimi, M.S., Fathizadeh, H., et al., 2021. Chitosan-based nanoparticles against bacterial infections. Carbohydr. Polym. 251 (September 2020), 117108.

Rifabutin Uses, Side Effects & Warnings - Drugs.com [Internet]. [citado 30 de diciembre de 2022]. Disponible en: https://www.drugs.com/mtm/rifabutin.html.

Rinaudo, M., 2006. Chitin and chitosan: properties and applications. Prog. Polym. Sci. 31 (7), 603–632.

Robla, S., Prasanna, M., Varela-Calviño, R., Grandjean, C., Csaba, N., 2021. A chitosan-based nanosystem as pneumococcal vaccine delivery platform. Drug Deliv. Transl. Res. 11 (2), 581–597.

Rockwood, N., Cerrone, M., Barber, M., Hill, A.M., Pozniak, A.L., 2019. Global access of rifabutin for the treatment of tuberculosis – why should we prioritize this? J. Int. AIDS Soc. 22 (7), 1–7.

Schön, T., Chryssanthou, E., 2017. Minimum inhibitory concentration distributions for Mycobacterium avium complex—Towards evidence-based susceptibility breakpoints. Int. J. Infect. Dis. 55, 122–124, 1 de febrero de.

Sousa, M., Pozniak, A., Boffito, M., 2008. Pharmacokinetics and pharmacodynamics of drug interactions involving rifampicin, rifabutin and antimalarial drugs. J. Antimicrob. Chemother. 62 (5), 872–878.

Tuoriniemi, J., Johnsson, A.C.J.H., Holmberg, J.P., Gustafsson, S., Gallego-Urrea, J.A., Olsson, E., et al., 2014. Intermethod comparison of the particle size distributions of colloidal silica nanoparticles. Sci. Technol. Adv. Mater. 15 (3).

Vila-Sanjurjo, C., David, L., Remuñán-López, C., Vila-Sanjurjo, A., Goycoolea, F.M., 2019. Effect of the ultrastructure of chitosan nanoparticles in colloidal stability, quorum quenching and antibacterial activities. J. Colloid. Interface Sci. 556, 592–605, 15 de noviembre de.

Woods, G.L., 2011. Susceptibility Testing of Mycobacteria, Nocardiae, and Other Aerobic Actinomycetes, 2nd edition. Clinical and Laboratory Standards Institute., p. 61

World Health Organization. Tuberculosis [Internet]. [citado 30 de diciembre de 2022]. Disponible en: https://www.who.int/news-room/fact-sheets/detail/tuberculosis.

Zhu, Y., Zhang, G., Yang, H., Hong, X, 2005. Influence of surfactants on the parameters of polylactide nanocapsules containing insulin. J. Surfactants Deterg. 8 (4), 353–358.